

A four-miRNA Signature as a Potential Biomarker of malignant mesothelioma patients from hand-spinning asbestos exposed area in Eastern China

Lijin Zhu

Hangzhou Medical College

Shibo Ying

Hangzhou Medical College

Xin Su

Hangzhou Medical College

Wenke Yu

Hangzhou Medical College

Kaili Yan

Hangzhou Medical College

Wei Shen

Cixi No. 3 People's Hospital

Shuaiyue Hu

Hangzhou Medical College

Zhaoqiang Jiang

Hangzhou Medical College

Hailing Xia

Hangzhou Medical College

Lingfang Feng

Hangzhou Medical College

Yan Zeng

Hangzhou Medical College

Junqiang Chen

Hangzhou Medical College

Xing Zhang

Hangzhou Medical College

Jianlin Lou

jianlinlou@163.com



Hangzhou Medical College

Research Article

Keywords: Asbestos exposure, MicroRNA, Mesothelioma, Asbestos-related Diseases, Biomarker, Human biomonitoring

Posted Date: March 11th, 2024

DOI: <https://doi.org/10.21203/rs.3.rs-4005667/v1>

License:   This work is licensed under a Creative Commons Attribution 4.0 International License.
[Read Full License](#)

Additional Declarations: No competing interests reported.

Abstract

Malignant mesothelioma (MM) is an aggressive malignant tumor of mesothelial origin that develops mainly in the parietal pleura or peritoneum and is strongly associated with asbestos exposure. MicroRNAs (miRNA) can be used as biomarkers in the *in vitro* diagnosis of tumors. To study the differential expression of miRNAs in MM patients and identify potential biomarkers for diagnosis, we sequenced miRNAs in MM formalin-fixed paraffin-embedded (FFPE) tumor tissue and compared it with adjacent normal tissue, and the expression of four miRNAs was validated using *in situ* hybridization. Moreover, the expression differences of these four miRNAs in the plasma were also compared between lung cancer (LC) patients, patients with pleural plaques (PP), asbestos-exposed (AE) subjects and healthy controls by qPCR. We found a total of 31 differentially expressed miRNAs in the tumor tissue of mesothelioma patients compared to the adjacent normal tissue, with 18 upregulated miRNAs and 13 downregulated miRNAs. The elevated expression of miR-19b, miR-26a, miR-26b, and miR-29a in FFPE tumor tissue was further validated in both the cytoplasm and the nucleus using fluorescence *in situ* hybridization (FISH) hybridization. Furthermore, the plasma expression levels of miR-19b and miR-29a in the mesothelioma group were significantly higher than those in any of the other four groups, and similar expression differences were found in miR-26a and miR-26b between the mesothelioma group and any other group except the LC group. Diagnostic value analysis indicated high sensitivity and specificity of these four miRNAs in distinguishing MM patients from PP patients, AE subjects, and healthy controls. Conclusively, miR-19b, miR-26a, miR-26b and miR-29a are potential blood biomarkers for the early or differential diagnosis of MM.

1. Introduction

Malignant mesothelioma (MM) is an occupational aggressive malignant tumor of mesothelial origin that develops in the parietal pleura or peritoneum and is strongly associated with a long latency of 20–40 years after asbestos exposure (Jiang et al., 2018; Mao et al., 2017; Zhai et al., 2021). MM is highly lethal in that the overall survival of MM patients remains very poor, with a median survival duration of 12 months. It is difficult to diagnose early and shows a limited response to conventional chemotherapy and radiotherapy. In China, asbestos consumption has increased steadily since the 1960s and the burden of disease attributable to asbestos is increasing in recent years (Chen et al., 2022). Work conditions in asbestos-related industries were poor, and exposure levels frequently exceed the occupational exposure limit. Many cases of MM may simply be misdiagnosed as other cancers, as there is no mandatory requirement for tissue verification or radiographs. This low incidence may be a reflection of reduced reporting rates or limitations in diagnostic accuracy. Therefore, it is crucial to find early diagnostic biomarkers for asbestos-induced MM.

It is well recognized that multiple genes regulated by microRNA (miRNA)-mediated posttranscriptional modifications are involved in the development of cancer. Therefore, the expression of a single gene may not reliably be used to predict the biological process of tumors. MicroRNA (miRNA) expression assays expand the scope of studying tumor biology by interrogating multiple target perturbations that are related

to key target molecules, which may be a better strategy to study MM because of the multiplicity of gene mutations and pathway deregulations that underlie its aggressiveness and resistance to therapy. Understanding the miRNAs that are involved in gene regulation and the effectors in downstream signaling will provide an opportunity to interrogate these miRNAs to develop biomarkers for diseases and will also provide a means to target the biological effects of the gene(s) of interest and certain undruggable molecules. Establishing signatures that are based on a constellation of upregulated (oncogenic) and downregulated (tumor suppressor) miRNAs that are unique to each patient will stratify newly diagnosed patients by risk and provide invaluable tools for personalized therapy.

Experimental evidence supports an increasing role of miRNAs in the molecular biology of MM and asbestos-exposed subjects. MM cell lines derived from MM patients fail to express miR-31, and reintroduction of miR-31 suppresses the cell cycle and inhibits the expression of multiple factors involved in cooperative maintenance of DNA replication and cell cycle progression (Ivanov et al., 2010). It has been suggested that miR-31 has the ability to inhibit the proliferation, migration, invasion, and clonogenicity of MM cells (Ivanov et al., 2010). Another finding is that the ectopic expression of miR-205 in MeT-5A (mesothelial cell line), H2452 (an epithelioid MM cell line) and MSTO-211H (a biphasic MM cell line) induced a significant reduction of ZEB1 and ZEB2 (mesenchymal markers) and a consequent upregulation of E-cadherin gene (epithelial markers) expression, and it also inhibited migration and invasion. miR-205 downregulation correlated significantly with both a mesenchymal phenotype and more aggressive behavior through its regulation of the epithelial to mesenchymal transition (EMT) (Fassina et al., 2012). Differentially expressed miRNAs such as miR-145 (Cioce et al., 2014), miR-16 (Reid et al., 2013), miR-126 (Tomasetti et al., 2012), and miR-625-3p (Kirschner et al., 2012) have been found in patients with mesothelioma; miR-3960, hsa-miR-4497, hsa-miR-4508, hsa-miR-6089, hsa-miR-6125, hsa-miR-326 6775-5p (Jia et al., 2019), miR-126 (Santarelli et al., 2011), miR-103 (Weber et al., 2012), miR-1281 (Bononi et al., 2016) and miR-30d (Ju et al., 2017) have also been found in asbestos-exposed subjects.

In this study, we evaluated the expression profiles of miRNAs in formalin-fixed paraffin-embedded (FFPE) cell blocks from three Chinese patients with MM and three nonmalignant matched tissues. Four miRNAs were selected for fluorescence in situ hybridization (FISH) verification and qPCR verification of plasma species and compared with those of lung cancer (LC) patients, pleural plaques (PP) patients, asbestos-exposed (AE) subjects and healthy controls. The receiver operating characteristic (ROC) curve and the target genes of the 4 miRNAs were analyzed.

2. Materials and Methods

2.1. Ethical considerations

This study was carried out in accordance with the Declaration of Helsinki and approved by the local ethics committee of the Hangzhou Medical College. The study protocol was explained to all study populations, and informed consent was provided by all study subjects.

2.2. Study population

The 85 FFPE MM tissue specimens from between 1998 and 2017 were retrospectively collected from several neighboring towns with a long history of hand-spinning asbestos industry in Southeast China (Gao et al., 2015; Jiang et al., 2018). Clinical information was obtained from the admission note of each hospital. The tissue sections were representative of the three histopathological types: fifty-seven epithelioid, four biphasic, and six sarcomatoid, and 18 unknown histopathological types were collected at diagnosis (patients did not receive previous treatments). The histology of mesothelioma was independently reviewed by two pathologists. Two biphasic and one epithelioid FFPE specimens from female nonsmokers aged 49–52 with asbestos exposure were used to construct a small RNA library for sequencing. The other 82 FFPE specimens were used for tissue microarrays (TMAs) and FISH.

A total of 196 plasma specimens were collected from this hand-spinning asbestos exposed area. The subjects were divided into 5 subgroups: (1) a control group of 50 healthy individuals who were not exposed to any type of asbestos and had normal chest X-ray results and (2) a group of 21 patients diagnosed with MM, (3) a group of 50 individuals with lung cancer (LC) alone, (4) a group of 25 patients diagnosed with PP, and (5) an AE group of 50 individuals who were occupationally exposed to asbestos without any imaging changes. There was no significant difference in the distribution of age, sex or the ratio of smokers among the 5 groups (Table 1). Data collection was carried out following previously described procedures (Ying et al., 2017). Briefly, all subjects underwent chest X-rays. Nonmalignant asbestos-related diseases (ARDs) were diagnosed following the American Thoracic Society (ATS) criteria (American Thoracic, 2004) in Hangzhou Medical College. Blood specimens of patients with confirmed malignant mesothelioma (MM) were collected from 2014 to 2020. The inclusion criteria were as follows: (1) MM diagnosed by at least two independent pathologists according to the Guidelines for Pathologic Diagnosis of Malignant Mesothelioma proposed by the International Mesothelioma Interest Group (Husain et al., 2018), (2) no chemotherapy prior to blood sampling, and (3) informed consent signed by MM patients or their lineal relatives. Patients who were diagnosed with other malignant tumors were excluded from our study. A venous blood sample was obtained from all participants at the time of diagnosis before receiving any treatment. Five milliliters of peripheral blood from each subject was collected into tubes containing ethylenediaminetetraacetic acid (EDTA). Tubes were centrifuged at 3000 rpm/min for 10 min at room temperature, and the supernatant was transferred into 1.5 ml centrifuge tubes (Axygen, USA) and stored at -80°C.

Table 1
General characteristics of the study subjects.

	Control (n = 50)	MM (n = 21)	LC (n = 50)	PP (n = 25)	AE (n = 50)
Age (years) (mean ± SD)	61.68 ± 3.10	62.00 ± 12.72	60.66 ± 4.93	62.64 ± 1.91	63.62 ± 1.85
Sex (male/female) [n(n%)]	23/27 (46%/54%)	9/12 (43%/57%)	22/28 (44%/56%)	10/15 (40%/60%)	14/36 (28%/72%)
Smoker [n%]	9 (18%)	4 (19%)	13 (26%)	4 (20%)	6 (12%)
Drinker [n%]	5 (10%)	0	11 (22%)	4 (20%)	1 (2%)
MM: malignant mesothelioma; LC: lung cancer; PP: pleural plaque; AE: asbestos exposed					

2.3. Small RNA library construction and sequencing

Three FFPE specimens from three epithelioid MM patients were used to construct the small RNA library for sequencing. Total RNA from the three FFPE specimens was extracted using TRIzol reagent (Invitrogen, CA, USA) following the manufacturer's instructions. Approximately 1 µg of total RNA was used to prepare a small RNA library according to the protocol of the TruSeq Small RNA Sample Prep Kit (Illumina, San Diego, USA). Then, we performed single-end sequencing (36 bp) on an Illumina Hiseq2500 at LC-BIO (Hangzhou, China) following the vendor's recommended protocol.

Data processing was performed according to the procedures described in a previous study (Li et al., 2010) provided by LC Sciences Service. Briefly, the raw reads were subjected to the Illumina pipeline filter (Solexa 0.3), and then the dataset was further processed using an in-house program, ACGT101-miR (LC Sciences, Houston, Texas, USA), to remove adaptor dimers, junk, low complexity, common RNA families (rRNA, tRNA, snRNA, snoRNA) and repeats. Subsequently, unique sequences with lengths of 18 ~ 26 nucleotides were mapped to specific species precursors in miRbase 20.0 using a BLAST search to identify known miRNAs and novel 3p- and 5p-derived miRNAs. Length variation at both the 3' and 5' ends and one mismatch within the sequence were allowed in the alignment. The unique sequences that mapped to specific species in mature miRNAs in hairpin arms were identified as known miRNAs. The unique sequences that mapped to the other arm of the known specific species precursor hairpin opposite the annotated mature miRNA-containing arm were considered novel 5p- or 3p-derived miRNA candidates. The remaining sequences were mapped to other selected species precursors (with the exclusion of specific species) in miRBase 20.0 by a BLAST search, and the mapped pre-miRNAs were further BLASTed against the specific species genomes to determine their genomic locations. The above two sequences were defined as known miRNAs. The unmapped sequences were BLASTed against the specific genomes, and the hairpin RNA structures containing sequences were predicated from the flanking 80 nt sequences using RNAfold software (<http://rna.tbi.univie.ac.at/cgi-bin/RNAfold.cgi>). The criteria for secondary structure prediction were as follows: (1) number of nucleotides in one bulge in the stem (≤ 12), (2) number of base pairs in the stem region of the predicted hairpin (≥ 16), (3) cut-off free energy

(kCal/mol ≤ 15), (4) length of hairpin (up and down stems + terminal loop ≥ 50), and (5) length of hairpin loop (≤ 20), (6) number of nucleotides in one bulge in the mature region (≤ 8), (7) number of biased errors in one bulge in the mature region (≤ 4), (8) number of biased bulges in the mature region (≤ 2), (9) number of errors in the mature region (≤ 7), (10) number of base pairs in the mature region of the predicted hairpin (≥ 12), and (11) percent of maturity in the stem (≥ 80).

miRNA differential expression based on normalized deep-sequencing counts was analyzed by selectively using Fisher's exact test, the chi-square 2×2 test, the chi-square $n \times n$ test, Student's t-test, and ANOVA based on the experimental design. The significance threshold was set to 0.05 in each test.

2.4. Tissue microarray (TMA) construction

The 82 FFPE MM tissue specimens were intraoperatively dissected from the mesothelioma tissue, and paired normal mesothelial tissue was obtained from the same patients. The TMAs (Superchip Biotech, Shanghai) were assembled using a tissue-arraying instrument (Beecher Instruments, Silver Springs, Md). Four tissue microarray blocks were made to include all the tissue samples. Multiple 4- μ m-sections were cut with a Micron microtome (HM355S) and stained for FISH analysis.

2.5. Fluorescence in situ hybridization (FISH)

The expression levels of miR-19b-3p, miR-26a-5p, miR-26b-5p, and miR29a-3p in tissues were evaluated by FISH using a specific digoxin-labeled miRNA probe on the TMAs. miRNAs were stained in the cytoplasm and the nucleus. The quantitative scanning approach to evaluate the staining and expression of miRNA was Aperio ImageScope V11 from Leica Company as described previously (Chabot-Richards et al., 2011), and the positivity value $\times 100$ represents the expression of miRNA. Representative effective tissue sections were scored semiquantitatively by light microscopy. The TMA cores were scored anonymously and independently by one experienced pathologist and one oncologist. The mean score for duplicate cores from each individual was calculated. We then categorized the staining into high and low expression. miRNA expression was scored based on the following criteria: 1, 0 points for no staining; 2, 1 point for $< 20\%$; 3, 2 points for $20\text{--}40\%$; 4, 3 points for $40\text{--}60\%$; 5, 4 points for $60\text{--}80\%$; and 6, 5 points for $> 80\%$ of tumor tissue stained, as described previously (Lin et al., 2014). Scoring intensities based on blue cytoplasmic staining were graded from 0–3 in tumor cells (0, none; 1, weak; 2, intermediate; and 3 strong). The total score was determined by the following formula: staining index = intensity \times positive rate. In the present study, a staining index ≤ 8 was considered low expression, and a staining index > 8 was considered high expression.

2.6. Real-time quantitative PCR of miRNA

A total of 196 plasma specimens from MM, LC, PP, AE and control subjects were used to quantify miRNA expression. miRNAs for real-time quantitative PCR (qRT-PCR) were isolated from 200 μ l of pooled plasma samples using the miRNeasy Mini Kit (Qiagen, CA) following the manufacturer's protocol and eluted in 14 μ l of RNase-free water. cDNA was generated using 2.5 μ l of RNA per reaction in conjunction with miR-19b, miR-26a, miR-26b, or miR-29a RT primers and a miRNA reverse transcription kit (TaKaRa

Technologies). Quantitative PCR (qPCR) was performed using SYBR Green qPCR master mix (TaKaRa). Expression levels for candidate miRNAs were normalized to U6. After normalization to U6 (ΔCt), the ΔCt values for miRNAs in controls were averaged and subtracted from the ΔCt values of each individual sample ($\Delta\Delta\text{Ct}$), and expression levels were calculated using the $2^{-\Delta\Delta\text{Ct}}$ method (Ju et al., 2017).

2.7. Receiver operating characteristic (ROC) curves

Predictive performance was assessed with respect to the ability of each miRNA to discriminate between MM cases, LC cases, PP cases, asbestos-exposed cases and controls, and the ROC curve was used to evaluate the true positive rate (sensitivity) on the y-axis and the false positive rate (1-specificity) on the x-axis. An area under the ROC curve of 1.0 indicates perfect discrimination, whereas an area with a confidence interval of 0.5 indicates that the discriminatory ability of the test was not better than that of random chance (Jiang et al., 2017). A two-sided $P < 0.05$ was considered statistically significant. Analyses were performed with GraphPad Prism 8.0 and SPSS Statistics 17.0 (SPSS Inc., Chicago, IL, USA).

2.8. Prediction of target genes of miRNAs

To predict the genes targeted by differentially expressed miRNAs, two computational target prediction algorithms, TargetScan 5.0 (<http://www.targetscan.org>) and miRanda 3.3a (<http://www.microrna.org/microrna/home.do>), were used to identify miRNA binding sites. Consensus targets predicted by the two algorithms were selected for enrichment analysis. Gene Ontology (GO) and Kyoto Encyclopedia of Genes and Genomes (KEGG) enrichment analyses were performed by David 6.7 (<http://david.abcc.ncifcrf.gov/home.jsp>). The GO categories and KEGG pathway categories analyzed by hypergeometric test with a 148 p-value less than 0.01 were retained.

3. Results

3.1. miRNA profiling in tumor tissues from MM patients

The results of miRNA sequencing are shown in Table 2 and Fig. 1. Based on the paired t-test, 84 miRNAs had significantly different expression levels between cancerous tissue and matched adjacent tissue ($P < 0.05$). When the number of reads was set to higher than 10, 30 known miRNAs and 1 novel miRNA displayed considerable expression differences between the two groups, with 18 upregulated miRNAs and 13 downregulated miRNAs (Fig. 1A and 1B).

We used the two current algorithms miRanda and TargetScan to map putative targets of mesothelioma dysregulated miRNAs; in total, 2710 genes were modulated by the 31 miRNAs. To identify the signaling pathways related to the genes and putative targets of dysregulated miRNAs, we performed GO (Fig. 1C) and KEGG analysis (Fig. 1D). Pathways of Wnt signaling, MAPK signaling, focal adhesion, calcium signaling, and chemokine signaling were found among the significant KEGG terms. Interestingly, all the target genes of the differentially expressed miRNAs are involved in cancer pathways.

Table 2

Expression of miRNAs measured by deep sequencing in which the number of reads was limited to greater than 10 for MM and matched adjacent tissues to cancer.

UP			DOWN		
miR_name	fold_ change	pvalue(t_test)	miR_name	fold_ change	pvalue(t_test)
hsa-miR-23b-3p	25.81	0.0438	hsa-miR-324-5p	0.82	0.0171
hsa-miR-26b-5p	5.55	0.00987	hsa-miR-652-3p	0.75	0.00142
mdo-miR-497-5p	3.66	0.0130	hsa-miR-1291	0.74	0.0273
hsa-miR-19b-3p	3.62	0.0227	hsa-miR-532-5p	0.70	0.0226
ola-miR-26	3.28	0.0468	hsa-miR-506-3p	0.58	0.0129
aca-let-7b-5p	3.28	0.0468	hsa-miR-146a-3p	0.54	0.0381
hsa-miR-27a-3p	3.17	0.0359	hsa-miR-106b-3p	0.42	0.0166
mo-miR-130a-3p	2.98	0.0147	hsa-miR-150-3p	0.41	0.0342
hsa-miR-497-3p	2.47	0.0488	hsa-miR-152-5p	0.39	0.0152
hsa-miR-130a-3p	2.25	0.00205	PC-3p-27208_86	0.38	0.0491
hsa-miR-590-5p	2.12	0.0340	hsa-miR-301a-5p	0.31	0.0202
hsa-miR-33a-5p	2.07	0.0402	hsa-miR-2277-3p	0.28	0.00836
hsa-miR-362-3p	1.96	0.0118	hsa-miR-22-3p	0.27	0.0339
hsa-miR-140-3p	1.86	0.0410			
hsa-miR-579-3p	1.78	0.03.17			
bta-miR-29e	1.72	0.000908			
hsa-miR-24-3p	1.71	0.0213			
mml-miR-130a-5p	1.61	0.0497			

3.2. Histopathological validation of selected miRNAs

There were 49 effective slicing pairs of MM samples with tumor and matched adjacent tissues in the TMA. The miRNA stained scoring intensities based on blue cytoplasmic staining were graded from 0 to 3 in tumor cells (Fig. 2A–2D). Positive miRNA expression was observed in more MM samples than in matched adjacent tissues. Specifically, cytoplasmic miR-19b, miR-26a and miR-29b were significantly upregulated in MM tissues compared with matched adjacent tissues, and nuclear miR-26b was significantly upregulated in MM tissues compared with matched adjacent tissues (Fig. 2E-2H).

3.3. Plasma miRNAs as potential biomarkers

To investigate whether the expression of the above 4 miRNAs is elevated in plasma from MM patients, we compared the plasma levels of these miRNAs among the five groups. As shown in Fig. 3, all 4 miRNAs were significantly upregulated in both the MM and LC groups compared with the control, PP, and AE groups. miR-26b was upregulated in the PP and AE groups compared with the control group. miR-29a and miR-19b were upregulated in the MM group compared with the LC group.

To further evaluate the diagnostic value of miRNAs in distinguishing MM patients from LC patients, patients with PPs, AE individuals, and healthy controls, the sensitivity and specificity of miRNAs were calculated. The areas under the curve (AUCs) for miR-19b, miR-26a, miR-26b, and miR-29a in distinguishing MM individuals from healthy controls were 0.89 (95% CI: 0.81–0.97), 0.96 (0.91–1.00), 0.97 (0.94–1.00), and 0.92 (0.86–0.98), respectively (Fig. 4). The AUCs for miR-26b in distinguishing PP individuals from healthy controls and AE from healthy controls were 0.87 (95% CI: 0.8–0.95) and 0.75 (0.65–0.84), respectively (Fig. 5). The AUC for miR-26b distinguishing PP individuals from AE was 0.68 (95% CI: 0.54–0.82). The AUCs of miR-19b and miR-29a for distinguishing MM from LC subjects were 0.67 (95% CI: 0.52–0.83) and 0.68 (95% CI: 0.54–0.82), respectively.

3.4. Pathway network of miRNAs and target genes

A network using CytoScape that includes the selected miRNAs (miR-19b-3p, miR-26a-5p, miR-26b-5p and miR29a-3p) with the predicted gene targets that were derived from the KEGG cancer pathways is shown in Fig. 5. The 4 upregulated miRNAs (red) target 154 genes. The CYCS, COL4A2, CDK6, SMAD4, CCDC6, GSK3B and TP53 genes were regulated by 3 of the 4 miRNAs, and the PTEN gene was regulated by 4 of the 4 miRNAs in the cancer pathway. The ZAK gene was regulated by 4 of the 4 miRNAs in the MAPK pathway, and the PPM1B, PPM1A, MAP3K2, MAP3K1, and RPS6KA6 genes were regulated by 3 of the 4 miRNAs in the MAPK pathway. The ACTN2, MYLK3, ITGA5 and VASP genes were regulated by 3 of the 4 miRNAs in the focal adhesion pathway.

4. Discussion

miRNAs-based biomarkers have significant advantages of reduced invasiveness, low cost, and highly sensitive, thereby represent a potential diagnostic index for a variety of diseases. In pathologic histology, there are increasing evidence regarding tissue and secreted miRNAs as biomarkers of MM and the biological characteristics associated with their potential diagnostic value (Han et al., 2021; Martinez-Rivera et al., 2018). In this study, we found the high expression of cytoplasmic miR-19b, miR-26a, and miR-29a, while nuclear miR-26a was significantly upregulated in MM tissues compared with matched adjacent tissues. Strikingly, among these 4 miRNAs, miR-19b and miR-26a in our study have been reported in MM cell lines or tissues in previous studies. Cappellesso et al. reported that miR-19b was overexpressed in MM cytological samples compared with benign/reactive pleurae and H2052 (epithelioid) and H28 (sarcomatoid) cell lines compared with the normal mesothelium cell line (MET-5A) (Cappellesso et al., 2016). Interestingly, Receiver-operating characteristic curve (ROC) analysis in MM

versus reactive mesothelial cells (RMC) showed that miR-19b has a high specificity of 0.90, but a low sensitivity of 0.42 in cytological samples (Cappellesso et al., 2016). As a potential histological diagnostic biomarker of MM, this high specificity but low sensitivity means those that are referred to miR-19b most often have MM (90%) but also many with MM are missed. In addition, Kirschner et al. found miR-26a-2-3p expressed in MM tissue is significantly lower than that in pericardial tissue samples served as control (Kirschner et al., 2012). Although the data are not completely consistent with our results when different control sample sources are used. Overall, the histological microRNAs miR-19b and miR-26a have been identified as potential diagnostic tool for MM, but their diagnostic accuracy in tissues is controversial and need for further investigation

Accumulating evidence also suggests the value of circulating miRNAs as possible blood-based biomarkers for MM. In our study, the usefulness of the 4 miRNAs miR-19b, miR-26a, miR-26b, and miR-29a as potential biomarkers for the diagnosis of MM from PP, AE, and control subjects was suggested. The plasma miR-19b and miR-29a levels also could serve as useful biomarkers for the diagnosis of MM from LC. Our study supports the notion that the 4 miRNAs miR-19b, miR-26a, miR-26b, and miR-29a are potential biomarkers to discriminate MM patients from asbestos-exposed patients with PP or healthy individuals. However, miR-26b is the only potential biomarker that can be discriminates among PP patients, AE patients and healthy individuals. miR-29a is the only potential biomarker that discriminates MM patients from LC. We combined the 4 miRNAs for analysis, but a higher AUC value was not obtained. The combination of miR-19b and miR-29a slightly increased the AUC value to discriminate MM patients from LC patients. From our perspective, miR-19b, miR-26a, miR-26b, and miR-29a can be used as blood biomarkers to supplement MM diagnosis. miR-26b may be a suitable blood biomarker to monitor occupational workers and their families who have a history of residential exposure to asbestos. The combination of miR-19b and miR-29a may be a blood biomarker for differentiating MM from LC. However, accurately discriminating MM and other carcinomas requires further investigation. Interestingly, among these 4 miRNAs, miR-26b and miR-29a in our study also have been reported in blood-based markers studies for Italian MM cohorts. Lamberti et al. found that miR-26b was overexpressed in the serum of patients compared with that of patients affected by noncancer-related pleural effusions, while miR-29a was detected exclusively in the serum of MPM patients (Lamberti et al., 2015). To our knowledge, our findings firstly validated the diagnostic value of these miRNAs from the tissue and blood specimen in patients with malignant mesothelioma in Chinese Han population.

In addition to the crucial roles of biomarkers, miRNAs also have been exploited as a novel therapeutic approach in MM. miRNAs have also been found to be associated with human cancers by interfering with the regulation of multiple tumor-related signaling pathways, such as oncogenes or tumor suppressor genes (Acunzo et al., 2015). Thereby, detailed targeted gene analysis may help to understand the possible role of these miRNAs in MM. Based on the results of miRNA-gene interaction analysis, we found in the cancer pathway, the PTEN gene is the predicted target gene of the 4 miRNAs, and the TP53 gene is the target gene of 3 of the 4 miRNAs, miR-19b, miR-26a, and miR-26b. PTEN is an important tumor suppressor that is located at chromosome 10q23. TP53 is also an important tumor suppressor that encodes the p53 protein. The mechanisms that regulate PTEN and TP53 are complicated and include

epigenetic silencing, transcriptional repression, miRNA regulation, disruption of competitive endogenous RNA (ceRNA) networks, posttranslational modifications, and aberrant localization (Lee et al., 2018; Song et al., 2012). Loss or decrease of PTEN is frequently observed in both heritable and sporadic cancers and is associated with a worse prognosis and metastases (Song et al., 2012). Even a small decrease (20%) in PTEN expression can dramatically influence the development of cancer (Alimonti et al., 2010; Carracedo et al., 2011). Interestingly, several studies have reported a link between TP53 and PTEN (Hamid et al., 2019; Martinez et al., 2022; Suwala et al., 2021), in which PTEN regulates the function of p53 by a phosphatase-dependent and phosphatase-independent mechanism (Freeman et al., 2003). It has been shown that PTEN is able to bind directly to TP53, increasing its stability and transcription (Salmena et al., 2008). It has also been known that the TP53 gene positively upregulates PTEN (Lee et al., 2018; Song et al., 2012). Although the roles of PTEN and TP53 is still controversial in MM (Agarwal et al., 2013; Bueno et al., 2016; Hmeljak et al., 2018), it was reported that PTEN expression is a strong predictor of survival for MM patients (Opitz et al., 2008). In addition, the PPM1B, PPM1A, MAP3K2, MAP3K1, and RPS6KA6 genes were regulated by 3 of the 4 miRNAs in the MAPK pathway, but the relationships of these genes and mesothelioma have not been reported. The MAPK pathway is involved in MM and is a potential target of MM gene therapy (Menges et al., 2012; Ou et al., 2011; Quispel-Janssen et al., 2018). It is possible that the differentially expressed miRNAs may take part in PTEN, TP53 expression and MAPK pathway. More research is needed to uncover the specific mechanisms of those miRNAs in pathway network.

This study had several strengths and some limitations. To our knowledge, this is the first study focusing on the non-coding RNA biomarker for MM in Chinese population. The previous studied cases of MM were mainly caused by crocidolite exposure. However, in our study the subjects of MM were from Eastern China, mainly caused by chrysotile exposure in occupational hand spinning. Thereby, the exposure sources are completely different from the other studies. Furthermore, our results were validated not only by tissues, but also by plasma sample. One limitation of this study is that we obtained only 82 FFPE samples and 23 plasma samples because MM is a malignant tumor with low incidence. The reason for the inconsistency of some findings with previous studies may be the small sample size or the different genetic features of other races. We combined multiple miRNAs to distinguish MM and LC patients, and the best AUC was 0.69 (0.56–0.83) when miRNA-19b was combined with miRNA-29a. More specific and sufficient blood biomarkers should be identified for the differential diagnosis of MM and other malignant tumors, especially LC. The mechanism of the signaling pathway of key molecules and their miRNA regulation needs further clarification.

5. Conclusions

In summary, we found that miR-19b, miR-26a, miR-26b and miR-29a may be biomarkers for MM diagnosis. These miRNAs possibly influence MM progression by targeting the PTEN and TP53 genes in cancer pathways. The MAPK signaling pathway may also be involved in MM progression. Future investigations should focus on the target genes of miR-19b, miR-26a, miR-26b and miR-29a and their regulatory mechanism, as well as on finding more miRNA biomarkers and their target genes.

Abbreviations

MM: Malignant mesothelioma; miRNA: MicroRNA; FFPE: formalin-fixed paraffin-embedded; LC: lung cancer; PP: pleural plaques; AE: asbestos-exposed; FISH: fluorescence in situ hybridization; ROC: receiver operating characteristic; TMAs: tissue microarrays; ARDs: asbestos-related diseases; ATS: American Thoracic Society; EDTA: ethylenediaminetetraacetic acid; qRT-PCR: real-time quantitative PCR; qPCR: quantitative PCR; GO: Gene Ontology; KEGG: Kyoto Encyclopedia of Genes and Genomes; AUC: area under the curve; RMC: reactive mesothelial cell; ceRNA: competitive endogenous RNA.

Declarations

Acknowledgements

Not applicable.

Author's Contributions

LJ.Z. and SB.Y. devised the main conceptual ideas. All authors contributed to drafting and revising the article and agree to be accountable for all aspects of the work. All authors read and approved the final manuscript.

Funding

This research was supported by National Natural Science Foundation of China (82273609, 81973011), the Hangzhou Medical College (Key Discipline of Zhejiang Province in Public Health and Preventive Medicine (First Class, Category A, KYYB202113, 26100548304-20), Zhejiang Provincial Department of Science and Technology (LGF21H260010), and Zhejiang Provincial Program for the Cultivation of High-level Innovative Health talents (2020).

Availability of data and materials

The data and study materials that support the findings of this study will be available to other researchers from the corresponding authors on reasonable request.

Ethics approval and consent to participate

All experiments were conducted in accordance with the Declaration of Helsinki and were approved by the Medical Ethics Committee of Hangzhou Medical College (LL2020-35).

Consent to publication

Not applicable.

Competing interests

The authors declare that there is no conflict of interest regarding the publication of this paper.

References

1. Acunzo M, et al. MicroRNA and cancer—a brief overview. *Adv Biol Regul.* 2015;57:1–9.
2. Agarwal V, et al. PTEN protein expression in malignant pleural mesothelioma. *Tumour Biol.* 2013;34:847–51.
3. Alimonti A, et al. Subtle variations in Pten dose determine cancer susceptibility. *Nat Genet.* 2010;42:454–8.
4. American Thoracic S. Diagnosis and initial management of nonmalignant diseases related to asbestos. *Am J Respir Crit Care Med.* 2004;170:691–715.
5. Bononi I, et al. Circulating microRNAs found dysregulated in ex-exposed asbestos workers and pleural mesothelioma patients as potential new biomarkers. *Oncotarget.* 2016;7:82700–11.
6. Bueno R, et al. Comprehensive genomic analysis of malignant pleural mesothelioma identifies recurrent mutations, gene fusions and splicing alterations. *Nat Genet.* 2016;48:407–16.
7. Cappellesso R, et al. Young investigator challenge: MicroRNA-21/MicroRNA-126 profiling as a novel tool for the diagnosis of malignant mesothelioma in pleural effusion cytology. *Cancer Cytopathol.* 2016;124:28–37.
8. Carracedo A, et al. PTEN level in tumor suppression: how much is too little? *Cancer Res.* 2011;71:629–33.
9. Chabot-Richards DS, et al. Quantitative image analysis in the assessment of diffuse large B-cell lymphoma. *Mod Pathol.* 2011;24:1598–605.
10. Chen J et al. 2022. A comparative study of the disease burden attributable to asbestos in Brazil, China, Kazakhstan, and Russia between 1990 and 2019. *BMC Public Health.* 22, 2012.
11. Cioce M, et al. Protumorigenic effects of mir-145 loss in malignant pleural mesothelioma. *Oncogene.* 2014;33:5319–31.
12. Fassina A, et al. Epithelial-mesenchymal transition in malignant mesothelioma. *Mod Pathol.* 2012;25:86–99.
13. Freeman DJ, et al. PTEN tumor suppressor regulates p53 protein levels and activity through phosphatase-dependent and -independent mechanisms. *Cancer Cell.* 2003;3:117–30.
14. Gao Z, et al. Asbestos textile production linked to malignant peritoneal and pleural mesothelioma in women: Analysis of 28 cases in Southeast China. *Am J Ind Med.* 2015;58:1040–9.
15. Hamid AA, et al. Compound Genomic Alterations of TP53, PTEN, and RB1 Tumor Suppressors in Localized and Metastatic Prostate Cancer. *Eur Urol.* 2019;76:89–97.
16. Han YQ, et al. Diagnostic value of microRNAs for malignant pleural mesothelioma: A mini-review. *Thorac Cancer.* 2021;12:8–12.

17. Hmeljak J, et al. Integrative Molecular Characterization of Malignant Pleural Mesothelioma. *Cancer Discov.* 2018;8:1548–65.
18. Husain AN, et al. Guidelines for Pathologic Diagnosis of Malignant Mesothelioma 2017 Update of the Consensus Statement From the International Mesothelioma Interest Group. *Arch Pathol Lab Med.* 2018;142:89–108.
19. Ivanov SV, et al. Pro-tumorigenic effects of miR-31 loss in mesothelioma. *J Biol Chem.* 2010;285:22809–17.
20. Jia J, et al. Genome-wide profiling reveals novel microRNAs in hand-spinning-specific chrysotile exposure. *Epigenomics.* 2019;11:511–25.
21. Jiang Z, et al. Hand-spinning chrysotile exposure and risk of malignant mesothelioma: A case-control study in Southeastern China. *Int J Cancer.* 2018;142:514–23.
22. Jiang Z et al. 2017. Plasma Fibulin-3 as a Potential Biomarker for Patients with Asbestos-Related Diseases in the Han Population. *Dis Markers.* 2017, 1725354.
23. Ju L, et al. miR-30d is related to asbestos exposure and inhibits migration and invasion in NCI-H2452 cells. *FEBS Open Bio.* 2017;7:1469–79.
24. Kirschner MB, et al. Increased circulating miR-625-3p: a potential biomarker for patients with malignant pleural mesothelioma. *J Thorac Oncol.* 2012;7:1184–91.
25. Lamberti M et al. 2015. Two Different Serum MiRNA Signatures Correlate with the Clinical Outcome and Histological Subtype in Pleural Malignant Mesothelioma Patients. *PLoS ONE* 10, e0135331.
26. Lee YR, et al. The functions and regulation of the PTEN tumour suppressor: new modes and prospects. *Nat Rev Mol Cell Biol.* 2018;19:547–62.
27. Li M, et al. MicroRNAome of porcine pre- and postnatal development. *PLoS ONE.* 2010;5:e11541.
28. Lin Y, et al. Identification and characterization of alphavirus M1 as a selective oncolytic virus targeting ZAP-defective human cancers. *Proc Natl Acad Sci U S A.* 2014;111:E4504–12.
29. Mao W, et al. Association of Asbestos Exposure With Malignant Mesothelioma Incidence in Eastern China. *JAMA Oncol.* 2017;3:562–4.
30. Martinez-Rivera V et al. 2018. Secreted and Tissue miRNAs as Diagnosis Biomarkers of Malignant Pleural Mesothelioma. *Int J Mol Sci* 19.
31. Martinez JD, et al. Common Genomic Aberrations in Mouse and Human Breast Cancers with Concurrent P53 Deficiency and Activated PTEN-PI3K-AKT Pathway. *Int J Biol Sci.* 2022;18:229–41.
32. Menges CW, et al. Group I p21-activated kinases (PAKs) promote tumor cell proliferation and survival through the AKT1 and Raf-MAPK pathways. *Mol Cancer Res.* 2012;10:1178–88.
33. Opitz I, et al. PTEN expression is a strong predictor of survival in mesothelioma patients. *Eur J Cardiothorac Surg.* 2008;33:502–6.
34. Ou WB, et al. AXL regulates mesothelioma proliferation and invasiveness. *Oncogene.* 2011;30:1643–52.

35. Quispel-Janssen JM, et al. Comprehensive Pharmacogenomic Profiling of Malignant Pleural Mesothelioma Identifies a Subgroup Sensitive to FGFR Inhibition. *Clin Cancer Res.* 2018;24:84–94.
36. Reid G, et al. Restoring expression of miR-16: a novel approach to therapy for malignant pleural mesothelioma. *Ann Oncol.* 2013;24:3128–35.
37. Salmena L, et al. Tenets of PTEN tumor suppression. *Cell.* 2008;133:403–14.
38. Santarelli L et al. 2011. Association of MiR-126 with soluble mesothelin-related peptides, a marker for malignant mesothelioma. *PLoS ONE* 6, e18232.
39. Song MS, et al. The functions and regulation of the PTEN tumour suppressor. *Nat Rev Mol Cell Biol.* 2012;13:283–96.
40. Suwala AK, et al. Glioblastomas with primitive neuronal component harbor a distinct methylation and copy-number profile with inactivation of TP53, PTEN, and RB1. *Acta Neuropathol.* 2021;142:179–89.
41. Tomasetti M, et al. Clinical significance of circulating miR-126 quantification in malignant mesothelioma patients. *Clin Biochem.* 2012;45:575–81.
42. Weber DG et al. 2012. Identification of miRNA-103 in the cellular fraction of human peripheral blood as a potential biomarker for malignant mesothelioma—a pilot study. *PLoS ONE* 7, e30221.
43. Ying S et al. 2017. Serum HMGB1 as a Potential Biomarker for Patients with Asbestos-Related Diseases. *Dis Markers.* 2017, 5756102.
44. Zhai Z et al. 2021. Assessment of Global Trends in the Diagnosis of Mesothelioma From 1990 to 2017. *JAMA Netw Open* 4, e2120360.

Figures

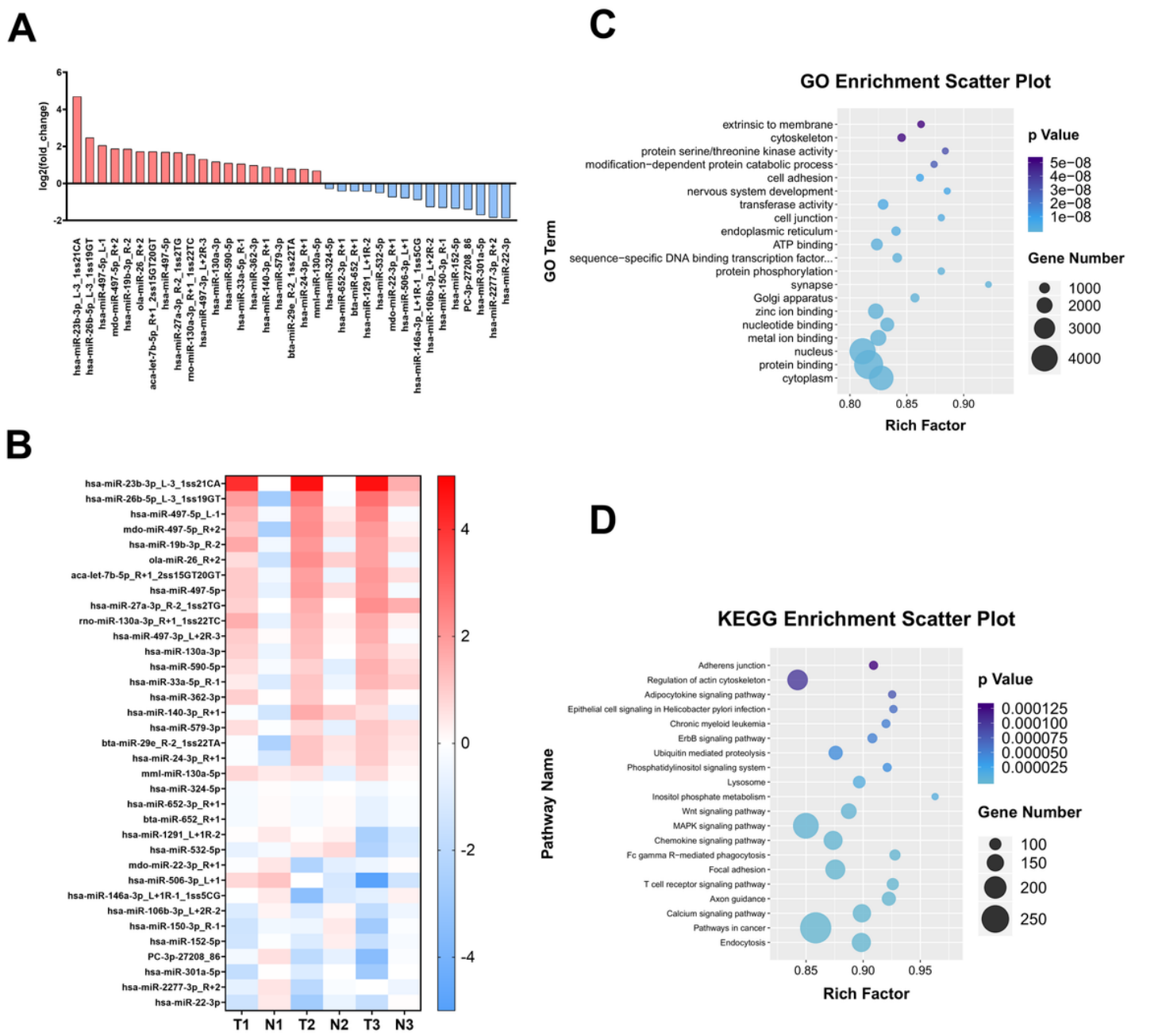


Figure 1

Deep sequencing analysis of miRNAs in MM and matched adjacent tissues and cancer and pathway enrichment analysis results of the target genes predicted by differentially expressed miRNAs predicted target genes. A, Expression of miRNAs measured by deep sequencing in which the number of reads was limited to greater than 10 for MM and matched adjacent tissues to cancer. Eighteen upregulated miRNAs (red bars) are shown above the x-axis, whereas 13 downregulated miRNAs (green bars) are shown below the x-axis. B, Heat map for differentially expressed miRNAs. The color represents the degree of expression; red represents upregulated miRNAs, while blue represents downregulated miRNAs. C: GO term enrichment. The dot size indicates the target gene number, and the color indicates the P-value. D: KEGG pathway enrichment. The dot size indicates the target gene number, and the color indicates the P-value.

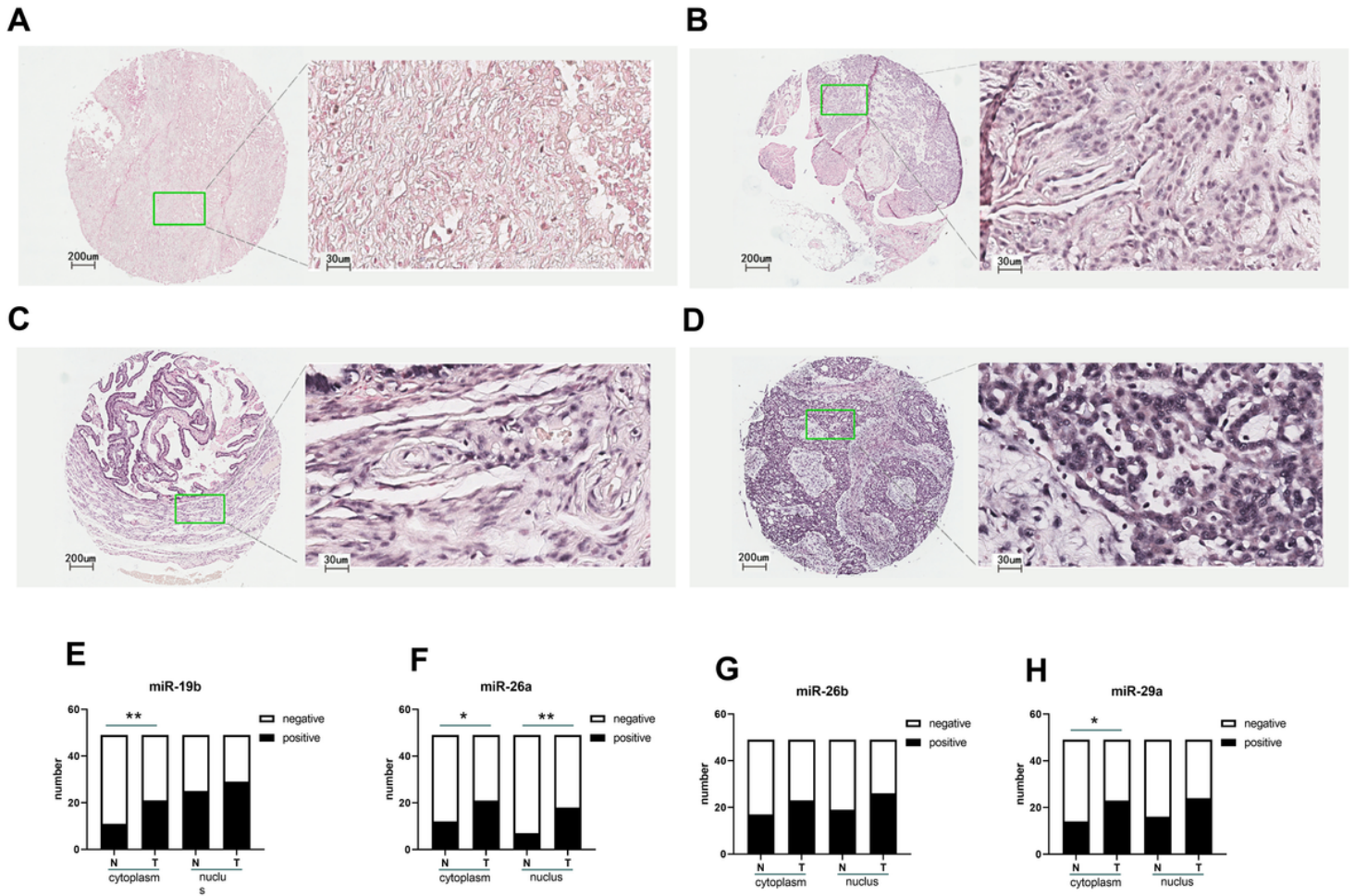


Figure 2

Fluorescence in situ hybridization (FISH) analysis of MM and paired normal mesothelial tissue. Scoring intensities based on blue cytoplasmic staining were graded from 0 to 3 in tumor cells. A: score 0; B: score 1; C: score 2; D: score 3. E: miR-19b expression in MM tissue and matched adjacent tissues; F: miR-26a expression in MM tissue and matched adjacent tissues; G: miR-26b expression in MM tissue and matched adjacent tissues; H: miR-29a expression in MM tissue and matched adjacent tissues. N: normal tissue, T: MM tissue; * $P < 0.05$, ** $P < 0.01$.

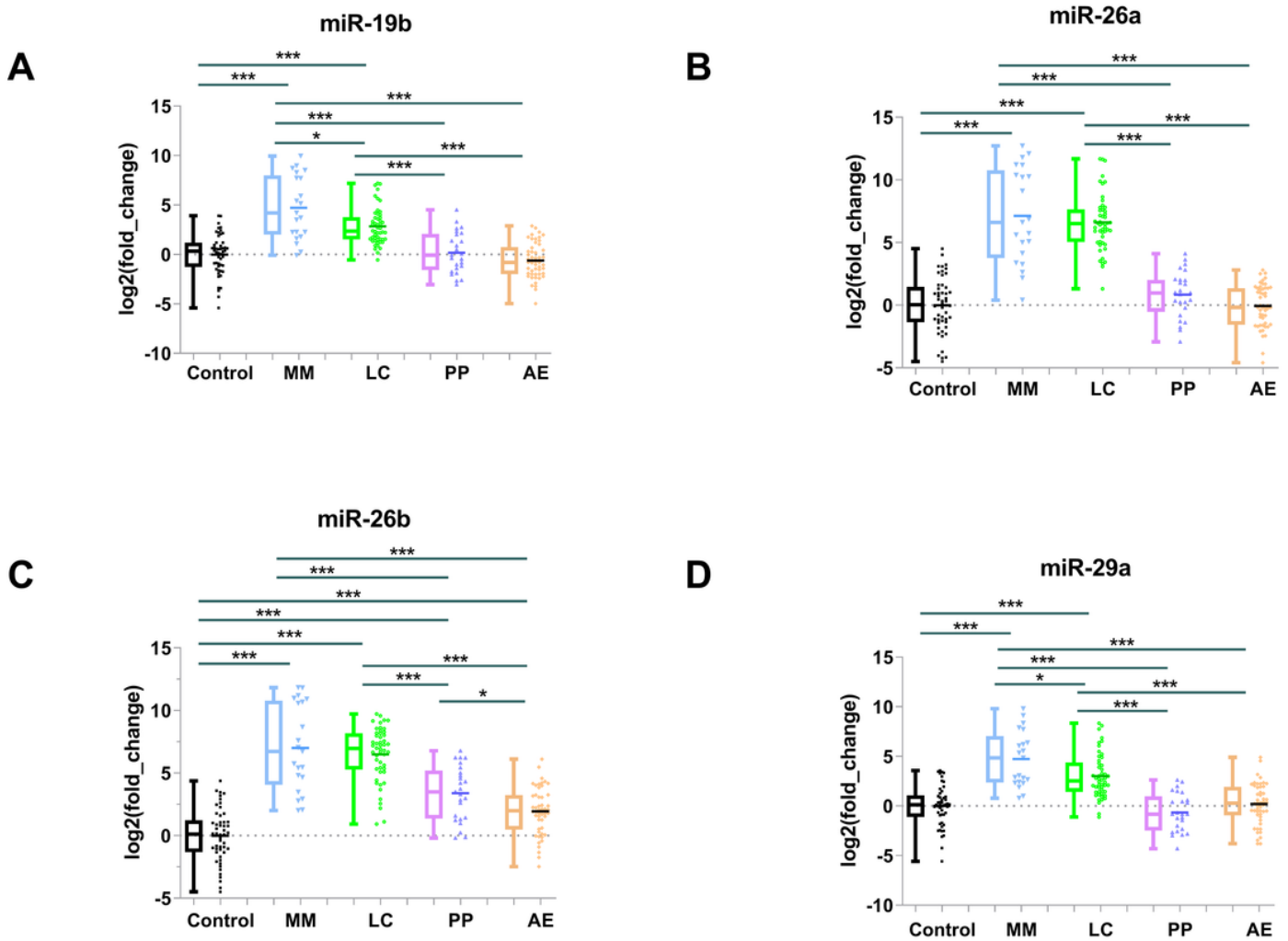


Figure 3

qRT-PCR analysis of miRNAs in the plasma of MM patients and LC, pleural plaque, AE individuals and healthy controls. A: miR-19b; B: miR-26a; C: miR-26b; D: miR-29a. *P < 0.05, **P < 0.01, ***P < 0.001.

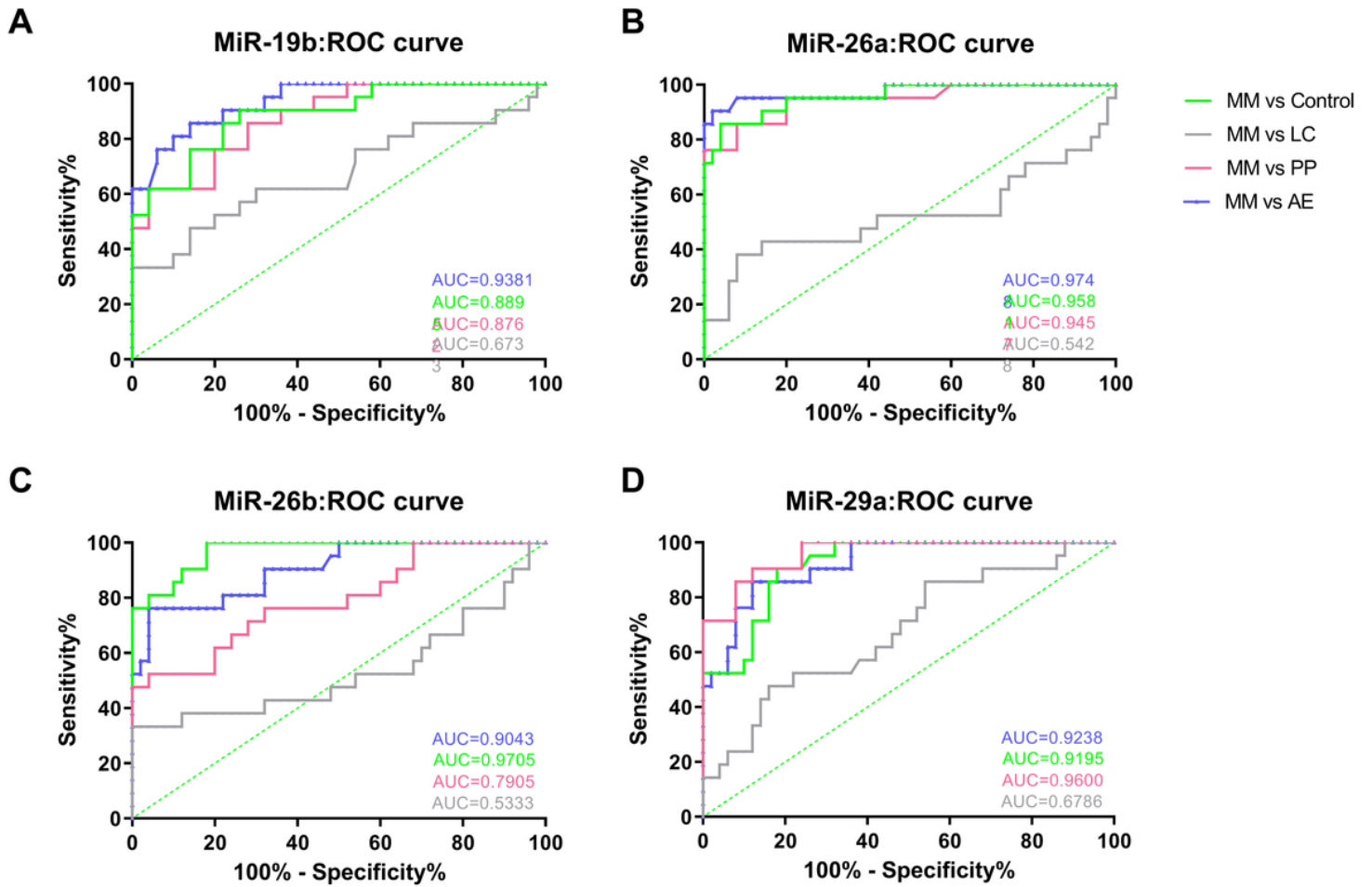


Figure 4

The ROC curves of miR-19b, miR-26a, miR-26b, and miR-29a for distinguishing MM individuals from LC, PP, AE and healthy controls. A: miR-19b; B: miR-26a; C: miR-26b; D: miR-29a.

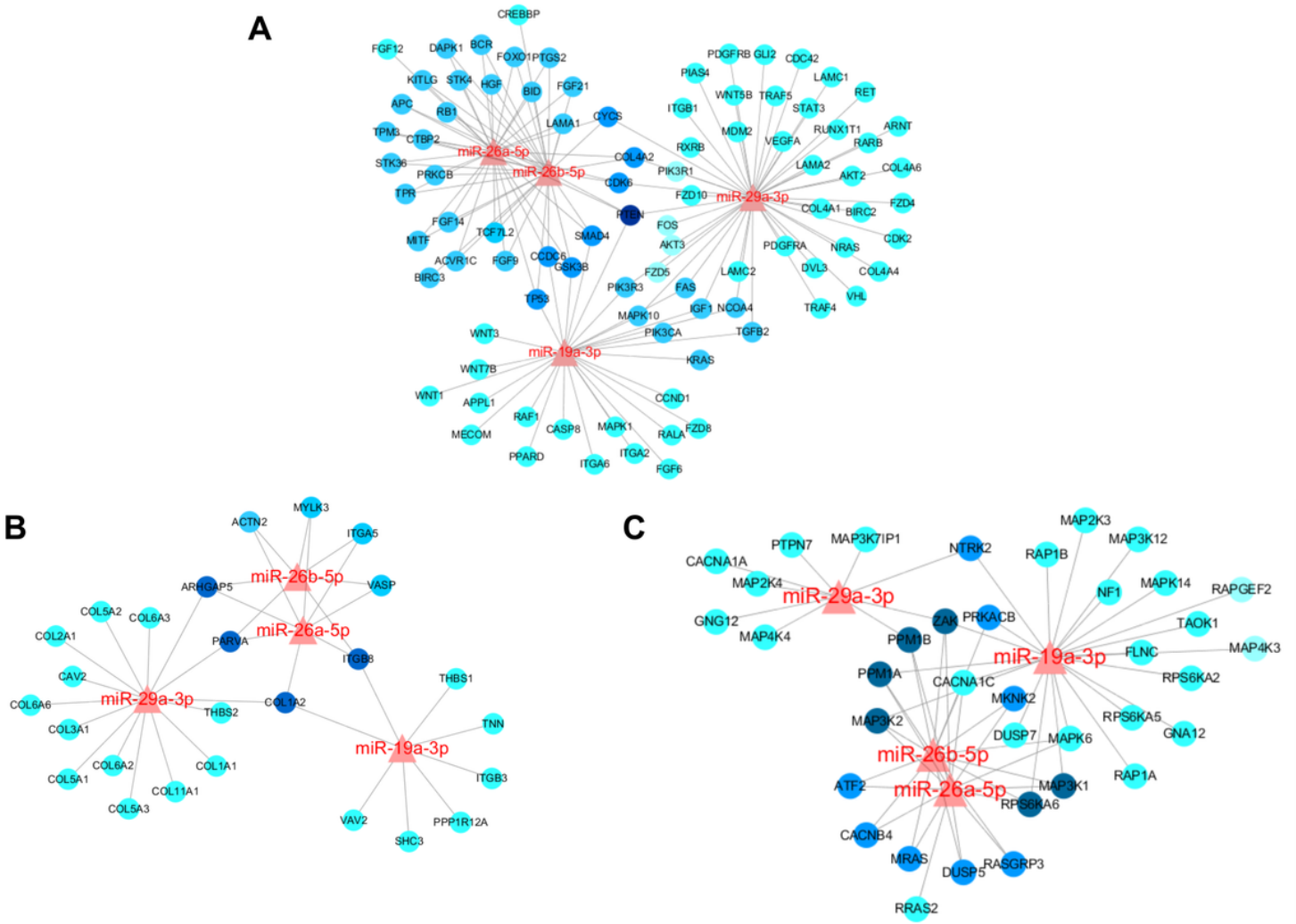


Figure 5

The miRNA-gene interaction network related to the signaling pathway of cancer, MAPK and focal adhesion. miR-19b-3p, miR-26a-5p, miR-26b-5p and miR-29a-3p with the predicted gene targets that were derived from the cancer pathway, focal adhesion pathway and MAPK pathway of the KEGG pathways. Red indicates a miRNA, and blue indicates cancer-related genes derived from the KEGG pathways. A: Pathway in cancer. B: Focal adhesion pathway. C: MAPK pathway.